

Affinity of six/seven glycomimetics for *Pseudomonas Aeruginosa* Lectin I determined in one experiment using a DNA glycoarray

Jing Zhang, Albert Meyer, Alice Goudot, Sonia Rouanet, Sébastien Vidal, Gwladys Pourceau, Jean-Pierre Cloarec, Jean-Pierre Praly, Eliane Souteyrand, Jean-Jacques Vasseur, Yann Chevotot*, François Morvan*

Supporting Information

1-Synthesis of glycomimetics G2-G7.....	1
2-Set up a DNA anchoring platform	10
3-Biological recognition	13
4-Figure for Hybridization and Cross Hybridization of the 7 glycomimetics.	14
5-Figure for Hybridization and Cross Hybridization of the 7 glycomimetics	15
6-F Molecular modelling protocol	17

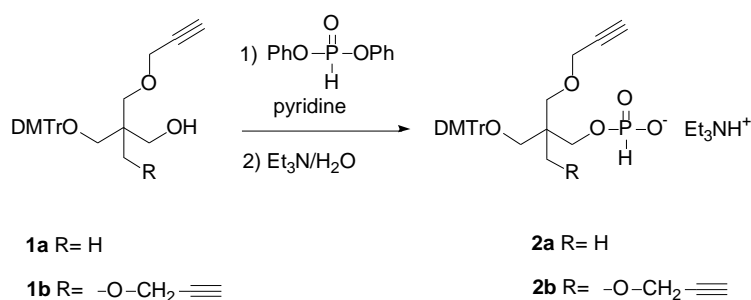
1-Synthesis of glycomimetics G2-G7

DNA tag of glycomimetics **G1-G7**

Glycomimetic	DNA tag Sequence 5' → 3'
G1	CTG CCT CTG GGC TCA
G2	GAA ACC AAG TCC ACA
G3	AGG AAA ACT GAG AAC AGA A
G4	TTG CTC GTT GAC CTC CAC T
G5	GCG ATA GAG CGT TCC TCC T
G6	CAA GTT GTC CAA TAC TTA T
G7	ACA CCA AAG ATG ATA TTT T

Firstly, we synthesized the *H*-phosphonate monoester derivatives bearing one or two propargyl groups starting from 1-*O*-(4, 4'-dimethoxytrityl)-2-propargyloxymethyl-2-methyl 1,3-propanediol¹ **1a** or 1-*O*-(4,4'-dimethoxytrityl)-2,2'-bis-propargyloxymethyl-1,3-propanediol² **1b** (Scheme 1). Each compound was treated with excess of diphenylphosphite and then the resulting phenyl *H*-phosphonate diester derivatives were hydrolyzed by water triethylamine affording the expected *H*-phosphonate monoester derivatives **2a** and **2b** respectively.

Scheme 1. General synthesis of mono and dipropargyl H-phosphonate monoester 3 and 4



Triethylammonium 1-O-(4, 4'-dimethoxytrityl)-2-propargyloxymethyl-2-methyl-3-O-hydrogenphosphonate-1,3-propanediol 2a

1-O-(4, 4'-dimethoxytrityl)-2-propargyloxymethyl-2-methyl 1,3-propanediol **1a** (690 mg, 1.5 mmol) was dried by azeotropic distillation with anhydrous pyridine (3×10 mL) and then dissolved in anhydrous pyridine (10 mL). Diphenylphosphite (2.05 mL 10.5 mmol, 7 eq.) was added and the mixture was stirred under argon for 1 hr at room temperature. After cooling ~ 5°C a mixture of water/triethylamine (10 mL 1:1 v/v) was added and stirred for 45 more min at rt. The crude was poured on a saturated bicarbonate solution (50 mL) and CH₂Cl₂ was added (50 mL). The organic layer was washed with saturated bicarbonate solution (2×50 mL), dried over Na₂SO₄ and evaporated to dryness. Crude product was purified by flash silica gel column chromatography (0 to 7% MeOH in CH₂Cl₂ containing 4% Et₃N) affording pure compound **2a** as a colourless oil (0.84 g, 90%). R_f= 0.13 (CH₂Cl₂/MeOH/Et₃N 92.5:5:2.5 v/v/v). ¹H NMR (CD₃CN, 300 MHz) δ: 0.95 (s, 3H, CH₃-C-(CH₂O)₃), 1.22 (t, J= 7.3 Hz, 9H, CH₃-CH₂-N), 2.72 (t, J=2.4 Hz, 1H, -C≡CH), 2.94 (s, 2H, -CH₂-ODMTr), 2.97 (q, J=7.3 Hz, 6H, -CH₂-N), 3.38 (s, 2H, -CH₂-O-CH₂-C≡CH), 3.63-3.66 (m, 2H, -CH₂-O-P), 3.79 (s, 6H, CH₃-O), 4.11 (d, J=2.4 Hz, 2H, -CH₂-C≡CH), 6.57 (d, 1H, J=597.6 Hz, H-P), 6.86-7.45 (m, 13H, Har). ¹³C NMR (CD₃CN, 75 MHz) δ: 7.6, 16.9, 40.0, 40.1, 45.0, 54.6, 57.8, 64.5, 65.8 (2), 72.3, 74.3, 79.8, 85.1, 112.6, 126.3, 127.4, 127.8, 129.8, 136.0, 145.2, 158.2. ³¹P NMR (CD₃CN, 121 MHz) δ: 2.55. HRESIMS (negative mode): *m/z* calcd for C₂₉H₃₂O₇P [M-Et₃NH]⁻ 523.1886, found 523.1894

Triethylammonium 1-O-(4, 4'-dimethoxytrityl)-2,2'-bis-propargyloxymethyl-3-O-hydrogenphosphonate-1,3-propanediol 2b

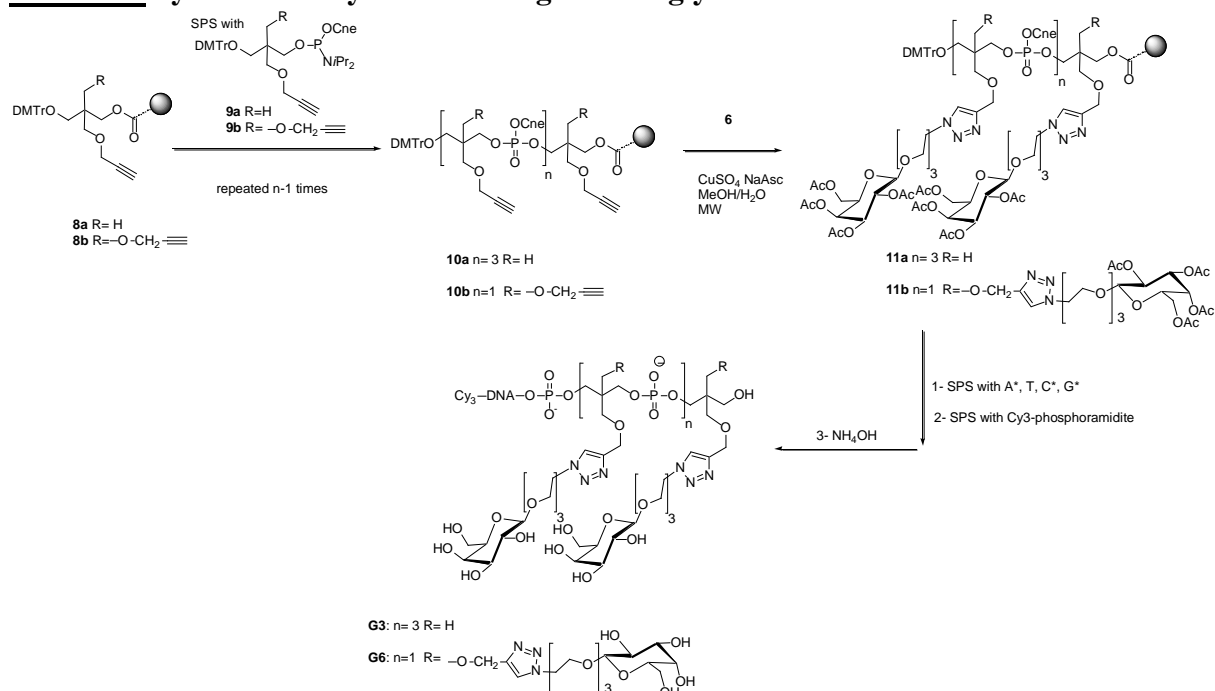
The same protocol was applied to 1-O-(4,4'-dimethoxytrityl)-2,2'-bis-propargyloxymethyl-1,3-propanediol **1b** (514 mg, 1 mmol) using 1.35 mL of diphenylphosphite (7 mmol, 7eq.). After purification, compound **2b** is obtained as a colourless oil (530 mg, 78%). R_f= 0.34

(CH₂Cl₂/MeOH/Et₃N 92.5:5:2.5 v/v/v). ¹H NMR (CD₃CN, 300 MHz) δ: 1.22 (t, J= 7.3 Hz, 9H, CH₃-CH₂-N), 2.73 (t, J=2.3 Hz, 2H, -C≡CH), 2.97 (q, J=7.3 Hz, 6H, -CH₂-N), 3.04 (s, 2H, -CH₂-ODMTr), 3.55 (s, 4H, -CH₂-O-CH₂-C≡CH), 3.73 (d, 2H, J=6.5 Hz, -CH₂-O-P), 3.79 (s, 6H, CH₃-O), 4.09 (d, J=2.4 Hz, 2H, -CH₂-C≡CH), 6.56 (d, 1H, J=599.8 Hz, H-P), 6.88-7.49 (m, 13H, Har). ¹³C NMR (CD₃CN, 75 MHz) δ: 7.6, 44.4 (2), 45.0, 54.6, 57.9, 61.0, 62.0, 68.8, 74.4, 79.7, 85.2, 112.6, 126.3, 127.4, 127.8, 129.8, 135.9, 145.1, 158.2. ³¹P NMR (CD₃CN, 121 MHz) δ: 2.54. HRFABMS (negative mode, thioglycerol): *m/z* calcd for C₃₂H₃₄O₈P [M-Et₃NH]⁻ 577.1991, found 577.1975

The other building blocks were already synthesized: DMCH *H*-phosphonate monoester **3**,³ propargyl-Thme **8a** and bis-propargyl-Pe **8b** solid, supports¹ propargyl-Thme **9a**⁴ and bis-propargyl-Pe **9b**² phosphoramidites and 1-Azido-3,6-dioxaoct-8-yl 2,3,4,6-tetra-*O*-acetyl-β-D-galactopyranoside **6**.⁵

Glycomimetic **G2** was synthesized according to the same protocol used for the synthesis of **G1** already described⁶ (Scheme 2). Basically starting from propanediol solid support, four DMCH *H*-phosphonate monoesters **3** were coupled by *H*-phosphonate chemistry using pivaloyl chloride as coupling agent. Propargylamine was introduced on each *H*-phosphonate diester by amidative oxidation using carbon tetrachloride in pyridine to give **5**. The four galactosyl residues were introduced by click chemistry under microwaves (MW) assistance using CuSO₄, sodium ascorbate and the tetraacetylated galactosyl triethylenglycol azide **6**. The oligonucleotide was then synthesized and labelled with fluorescent label (Cy3) by standard phosphoramidite chemistry. A final treatment with concentrated ammonia afforded the expected glycomimetic **G2**.

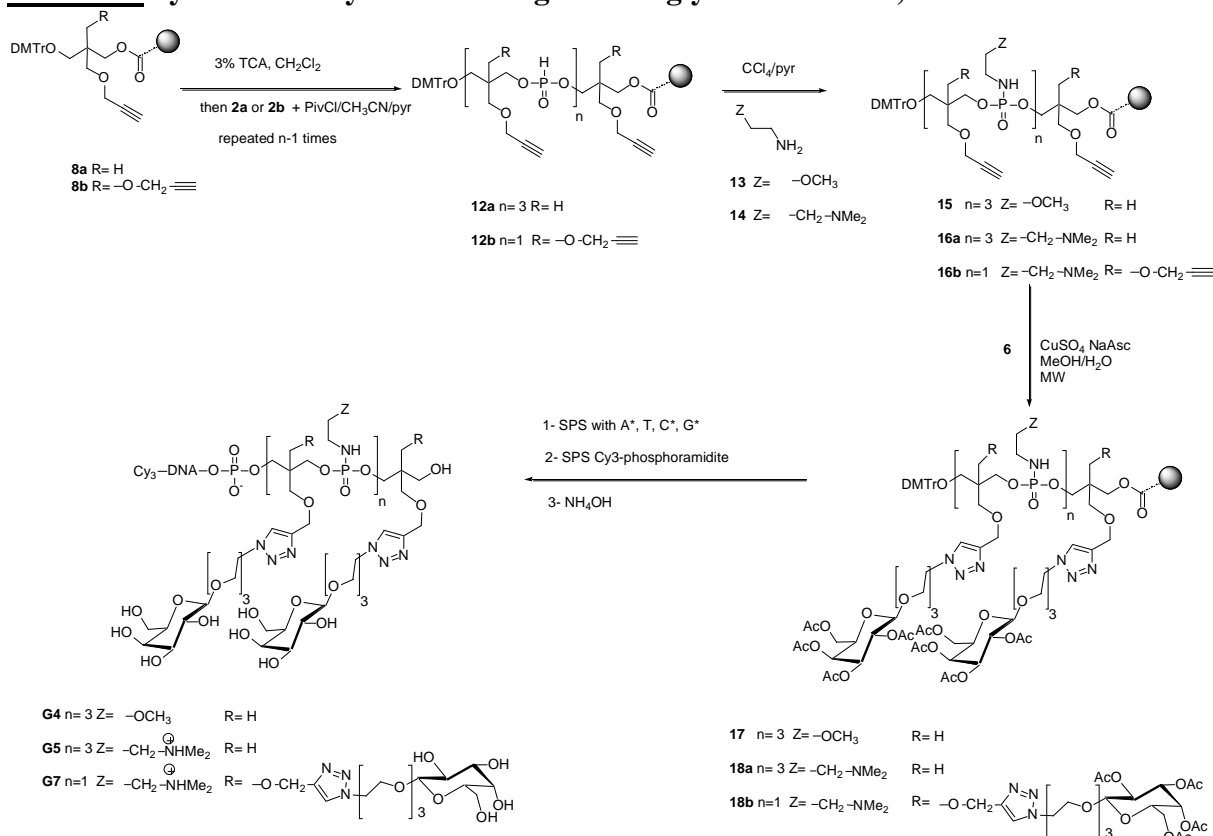
Scheme 3. Synthesis of Cy3-DNA-tetragalactose glycomimetic G3 and G6



Synthesis of linear neutral or positively charged glycomimetics G4 ThmePNMOE-Gal₄ and G5 ThmePNDMAP-Gal₄ and of antenna positively charged glycomimetic G7 PePNDMAP-Gal₄.

Starting from the mono propargylated **8a** or bis-propargylated **8b** solid supports, three mono-propargyl-Thme **2a** or one bis-propargylated-Pe **2b** *H*-phosphonate monoesters were coupled by *H*-phosphonate chemistry. The resulting tetraalkyne scaffolds exhibiting *H*-phosphonate diester linkages were oxidized by CCl₄ in presence of methoxyethylamine **13** or *N,N*-dimethylaminopropylamine **14** leading to **15**, **16a** and **16b** with phosphoramidate linkages. The galactose residues were introduced by click chemistry and the oligonucleotides were synthesized and labelled with Cy3 affording after ammonia treatment the expected linear and neutral glycomimetic **G4** and linear or antenna positively charged glycomimetics **G5** and **G7** respectively.

Scheme 4. Synthesis of Cy3-DNA-tetragalactose glycomimetic G4, G5 and G7



General procedure for introduction of alkyne functions using DNA chemistry

-by phosphoramidite chemistry:

The solid-supported phosphotriester tetraalkyne scaffolds **10a** and **10b** were synthesized at the $1\ \mu\text{mol}$ -scale on a DNA synthesizer (ABI 394) by standard phosphoramidite chemistry. For the coupling step, benzylmercaptotetrazole was used as activator (0.3 M in anhydrous CH₃CN) monoalkyne **9a** or dialkyne **9b** phosphoramidites (0.075 M in anhydrous CH₃CN) were introduced with a 60 s coupling time. The capping step was performed with acetic anhydride using commercial solution (Cap A: Ac₂O, pyridine, THF 10/10/80 and Cap B: 10% *N*-methylimidazole in THF) for 15 s. Oxidation was performed with commercial solution of iodide (0.1 M I₂, THF, pyridine/water 90/5/5) for 13s. Detritylation was performed with 2.5% DCA in CH₂Cl₂ for 35 s.

-by hydrogenophosphonate chemistry:

The solid-supported hydrogenophosphonate diester scaffolds **4**, **12a** and **12b** were synthesized at the $1\ \mu\text{mol}$ -scale on a DNA synthesizer (ABI 394). *H*-phosphonate monoesters **2a**, **2b** or **3** (0.06 M in anhydrous CH₃CN/C₅H₅N 1:1 v/v) were coupled using a *H*-phosphonate chemistry cycle with pivaloyl chloride as activator (200 mM in anhydrous CH₃CN/C₅H₅N 1:1 v/v). Each

solution was passed 6 times through the column alternatively for 5 s, (20 molar excess). Detritylation was performed with 2.5% DCA in CH₂Cl₂ for 35 s.

General procedure for amidative oxidation

The solid-supported *H*-phosphonate diesters scaffolds **4**, **12a** and **12b** (1 μmol) were treated back and forth using two syringes, with 2 mL of a solution of 10% of propargylamine **8**, 2-methoxyethylamine **13** or 3-dimethylamine-1-propylamine **14** (1000 eq. of NH₂ per *H*-phosphonate monoester) in CCl₄/C₅H₅N (1:1 v/v) for 30 min. The CPG beads were washed with C₅H₅N (2 × 2 mL) and CH₃CN (3 × 2 mL) and then dried by flushing with argon.

General procedure for Cu(I)-catalyzed 1,3-dipolar cycloaddition

To the solid-supported tetraalkyne scaffolds **5**, **10a**, **10b**, **15**, **16a** and **16b** were added acetylated galactosyl azide **6** (32 μL of a 0.5M solution in MeOH, 16 μmol, 4 eq. per alkyne function), freshly prepared aqueous solutions of copper sulfate (8 μL of 0.1M solution in H₂O) and sodium ascorbate (16 μL of a 0.25M solution in H₂O), 76 μL of water and 68 μL of MeOH. The tube containing the resulting preparation was sealed and placed in a microwave synthesizer Initiator from Biotage with a 30 s premixing time for 45 min at 60°C. Solution was removed and the CPG beads were washed with H₂O (3 × 2 mL), MeOH (3 × 2 mL) and CH₃CN (3 × 2 mL) and then dried by flushing with argon.

General procedure for elongation of DNA sequences and labeling with Cy3

The DNA sequences were synthesized on the solid-supported tetragalactose scaffolds **7**, **11a**, **11b**, **17**, **18a** and **18b** using standard phosphoramidite chemistry cycle like described above (see Generale procedure for introduction of alkyne functions using DNA chemistry by phosphoramidite chemistry). Commercially available nucleosides phosphoramites (A, T, C, G; 0.075 M in dry CH₃CN) were introduced with a 20 s coupling step whereas commercially Cy3 phosphoramidite (0.067 M in dry CH₃CN) was introduced with a 180 s coupling step.

General procedure for deprotection

The solid-supported oligonucleotide glycoconjugates were treated back and forth using two syringes, with 1 mL of concentrated aqueous ammonia for 30 min, then twice 0.5 mL for 30 min. For each compound, the solutions were withdrawn, warmed to 50°C for 2h, stirred at room temperature overnight and evaporated to dryness. Residues were dissolved in water and purified by reversed-phase preparative HPLC.

Analyses and Characterization of the Cy3-DNA-tetragalactose glycomimetics G2-G7

Compound G2:

HPLC RT=17.8 min; MS MALDI-TOF⁻ *m/z* calcd for C₂₇₀H₃₇₃N₈₀O₁₃₄P₂₀ [M-H]⁻: 7502.8 found 7503.9; 17 nmol calculated by UV measurement at 260 nm.

Compound G3:

HPLC RT=12.2 min; MS MALDI-TOF⁻ *m/z* calcd for C₂₉₇H₄₀₇K₁N₁₀₂O₁₅₈P₂₃ [M+K⁺-2H]⁻: 8685.5 found 8687.4; 30 nmol calculated by UV measurement at 260 nm.

Compound G4:

HPLC RT=13.2 min; MS MALDI-TOF⁻ *m/z* calcd for C₃₀₁H₄₃₅N₇₇O₁₇₃P₂₃ [M-H]⁻: 8612.5 found 8612.4; 52 nmol calculated by UV measurement at 260 nm.

Compound G5:

HPLC RT=11.1min; MS MALDI-TOF⁻ *m/z* calcd for C₃₀₈H₄₄₈N₈₈O₁₆₇P₂₃ (M-H)⁻: 8767.7 found 8766.6; 69 nmol calculated by UV measurement at 260 nm.

Compound G6:

HPLC RT=12.6 min; MS MALDI-TOF⁻ *m/z* calcd for C₂₈₅H₃₉₂N₈₀O₁₆₁P₂₁ [M-H]⁻: 8165.1 found 8164.4; 70 nmol calculated by UV measurement at 260 nm.

Compound G7:

HPLC RT=17.0 min; MS MALDI-TOF⁻ *m/z* calcd for C₂₉₁H₄₀₃N₈₇O₁₅₇P₂₁ [M-H]⁻: 8282.3 found 8279.2; n= 30 nmol calculated by UV measurement at 260 nm.

General remarks on HPLC analysis, purification and MS characterization

High performance liquid chromatography (HPLC) purifications and analyses were performed on a Waters Millipore instrument equipped with a reodyn injector a 600S controller and a Model 996 photodiode array detector. For analyses, a reverse phase C18 Nucleosil (5 μm) column (150 × 4.6 mm; Macherey-Nagel, Germany) was used at a flow rate of 1 mL min⁻¹ using a linear gradient of acetonitrile 16% to 40% in 0.05 M aqueous triethylammonium acetate (TEAAc) pH 7 for 30 min (except for the 26: 6 to 60% of acetonitrile in TEAAc for 25 min). For purifications, a reverse phase C18 Delta Pak (15 μm) column (7.8 × 300 mm; Waters, Japan) was used at a flow rate of 2 mL min⁻¹ using a linear gradient of acetonitrile 12% to 32% in 0.05 M aqueous triethylammonium acetate (pH 7) for 30 min (except for 26: 16% to 36% of acetonitrile in TEAAc for 20 min).

MALDI-TOF mass spectra were recorded on a Voyager mass spectrometer (Perspective Biosystems, Framingham, MA) equipped with a nitrogen laser. MALDI conditions were:

accelerating voltage 24000V; guide wire 0.05% of the accelerating voltage; grid voltage 94% of the accelerating voltage; delay extraction time 700 ns. 1 μL of sample was mixed with 5 μL of a saturated solution of THAP (except for **26**: HPA) in acetonitrile/water (1:1, v/v) containing 10% of ammonium citrate and few beads of DOWEX 50W-X8 ammonium sulfonic acid resin were added. Then, 1 μL of the mixture was placed on a plate and dried at room temperature and pressure.

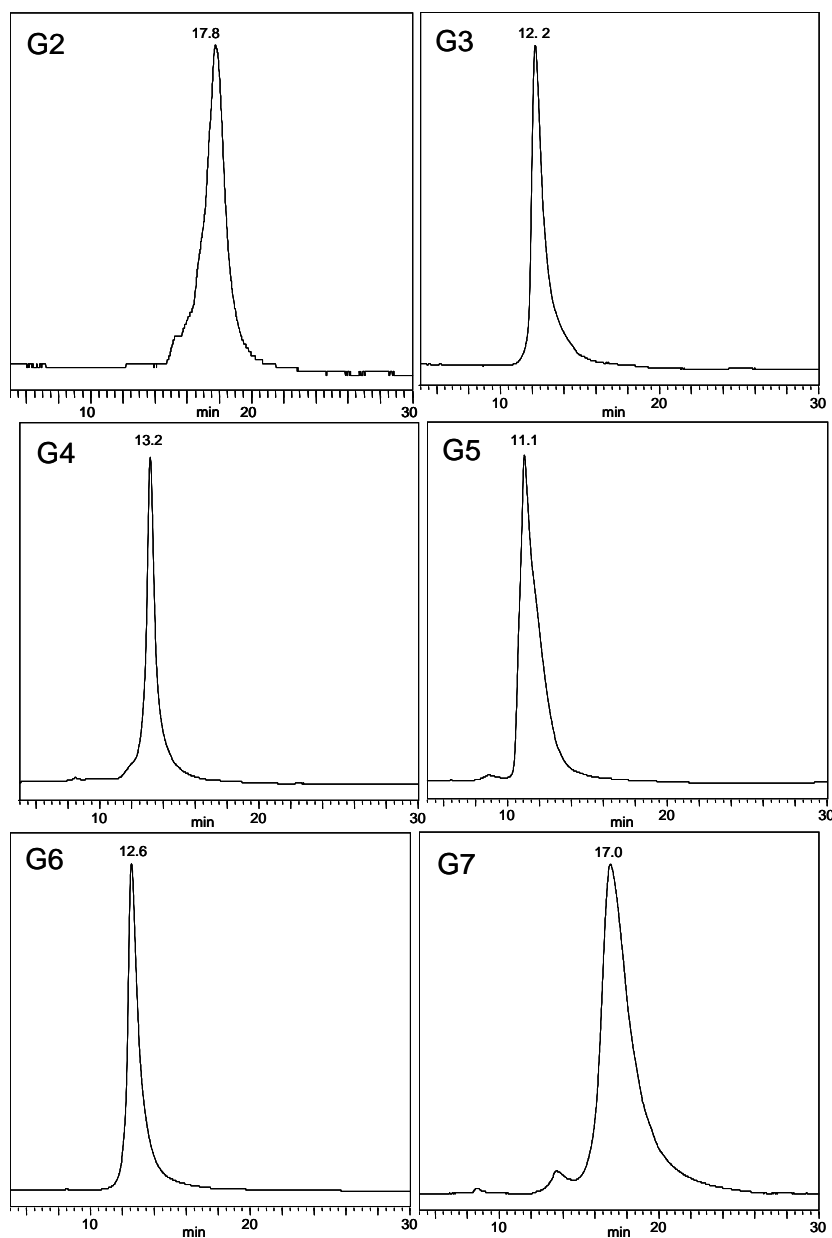


Figure 1: HPLC profiles of Cy3-DNA-glycomimetics G2-G7

2-Set up a DNA anchoring platform

The glass slides (Borosilicate, Nexterion D, Schott GMBH, Germany) were used as substrate supports (Figure 2). The setting up of the anchoring platform comprises three steps:

1. Fabrication of microreactors onto glass slides by photolithography and wet etching.^{7,8}
2. Surface chemical functionalisation of the supports leading to NHS ester activated glass slides.^{9,10}
3. Covalent immobilisation of amino-modified oligonucleotides acting as anchoring points for the subsequent immobilisation of the glycoconjugates.

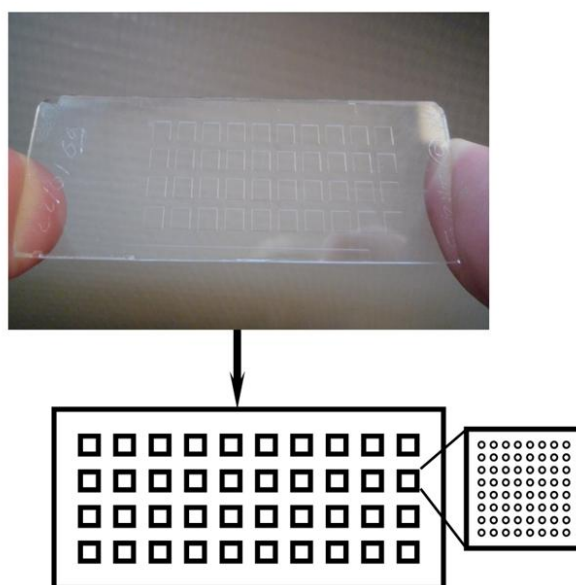


Figure 2: Photo and sketch map of the substrates. Glass slide featured 40 square microreactors.

Fabrication of microreactors (Substrate preparation)

Microreactors are designed onto flat glass slides by means of photolithography and wet etching. Technology process of the microreactor fabrication was adapted from the protocol developed by Mazurczyk et al.⁷ The process flow is shown in Figure 3.

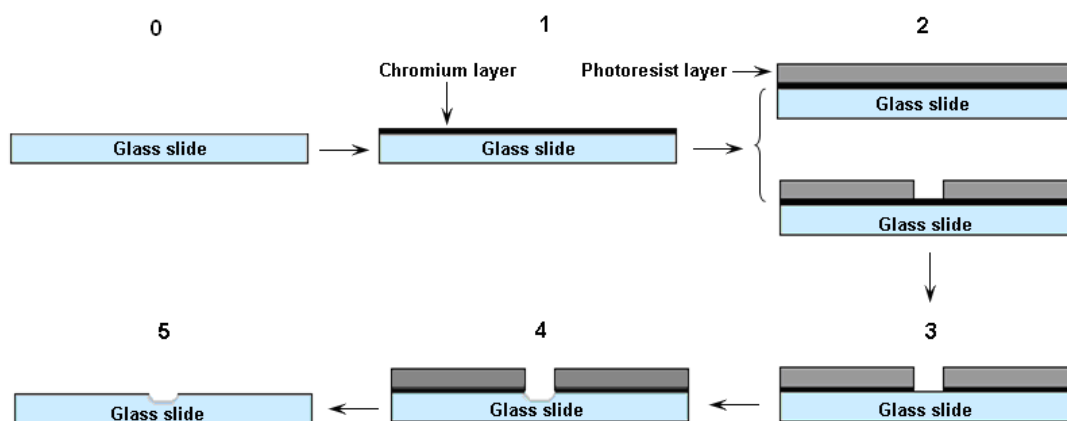


Figure 3. Technology processes of microreactors fabrication. 0. The original glass slide. 1. The deposition of a chromium layer. 2. A photolithographic step. 3. Opening of the chromium. 4. Glass etching. 5. Removing of the protective layers.

Deposition of the Chromium layer

Before photolithography, a chromium layer was deposited on the surface of the slide, in order to promote the adhesion of photoresist film with the slide and offer an additional protection against harsh etching solutions⁷. Firstly, the glass slides were washed successively with TDF4 detergent (Franklab SA, Billancourt, France) solution, a fresh Piranha mixture (96 % Sulphuric acid (Riedel de Haen, Puriss, Seelze, Germany): 35 % hydrogen peroxide (Fluka, Puriss, Steinheim, Germany), 7:3 volume) for 10 min, then rinsed with DI water (18.2 M Ω) and dried by centrifugation. A 150 nm chromium layer was deposited using magnetron sputtering (MRC822 system). The system was operated at a RF power of 5 kW, reflected power was 2 W, and turret voltages 2.6 kV. The argon flux was set to 50 sccm and the working pressure was $2.6 \cdot 10^{-3}$ Torr.

Photolithography

SPR 220 4.5 photoresist (Rohm Haas electronic materials, Lucerne, CH) was spin-casted at 4 000 rpm for 30s resulting in a 4 μ m thick layer. A first bake at 115 °C on a hot plate for 1 min 30 seconds was performed. Photolithography was carried out with a Karl Suss MJB3 Mask Aligner, and a 22 second illumination was performed. The slides were immersed in MF26 A developer for 1 minutes, rinsed in running DI water for 5 min, dried under a dry nitrogen flux and post-baked at 115°C for 2 minutes.

Etching

The chromium windows on the glass slides were opened using chromium etchant (Merck, Darmstadt, Germany). The slides were then rinsed in running DI water for 15 minutes and immersed in a freshly prepared wet etching solution (Buffered Oxide Etchant - abbreviated BOE, 7/1, Hydro fluoridric acid: ammonium fluoride, Honeywell): 37%hydrochloric acid (HCl, Riedel de Haen, Seelze, Germany): DI water (H₂O, 18.2 MΩ), 1/2/2, v/v/v) at room temperature for 1h and 15 minutes. The slides were rinsed in running DI water for 15 minutes. Complete removal of the photoresist was achieved by rinsing with acetone (Riedel de Haen), ethanol and water. Finally, the chromium layer was removed with chromium etchant (Merck, Darmstadt, Germany). Depth of the microwells was monitored with a mechanical profiler (Alfa-step 500 from KLA Tencor).

Silanisation and Activation of the glass slides

The microfabricated slides were washed with fresh Piranha solution for 20 min, and rinsed in deionized water for 10 minutes/4 times and dried by centrifugation. After heating the slides under dry nitrogen for 2 h at 150 °C in a sealed reactor, 250ml dry pentane was added at room temperature, followed by 300μL of tert-butyl-11-(dimethylamino)silylundecanoate. After incubation at room temperature under dry nitrogen for 2 hours, pentane was evaporated under reduced pressure and the slides were heated at 150 °C overnight and then washed in Tetrahydrofuran (THF, Riedel de Haen, Seelze, Germany) 10 minutes under sonication and rinsed with DI water. The tert-butyl ester was converted into the corresponding carboxyl group by immersing the slides in glacial formic acid (Riedel de Haen, Seelze, Germany) for 7 h at room temperature, washed successively 10 min in Dichloromethane (Sonication) and 10 minutes in water sonication. NHS activation of the carboxylic functions for the covalent immobilization of the amino-modified oligonucleotides was performed as follow: The glass slides were immersed in N-hydroxysuccinimide (Riedel de Haen, Seelze, Germany) 0.1 M and di(isopropyl)carbodiimide (Riedel de Haen, Seelze, Germany) 0.1 M in dry THF solution and allowed to react overnight at room temperature. Finally, the slides were rinsed successively in THF 10 minutes and dichloromethane 10 minutes under sonication leading to the NHS activated glass slides.

Immobilization of single-strand DNA

All amino modified DNA sequences were purchased from Eurogentec and prepared for fabrication of DNA anchoring platforms. Slide contained 40 square microreactors, each

microreactor has been used as a microchip. The amino modified nucleotides were deposited by a Biorobotics MicroGrid II microarrayer (Digilab), resulting 56 or 64 spots per well. Amino-oligonucleotides were printed from a 25 μM solution in PBS.

After deposition, the oligonucleotides were allowed to react with the carboxylic activated glass slides overnight at room temperature in a water vapor saturated chamber, and then the solutions were slowly evaporated overnight at room temperature. Finally, the slides were washed with 0.1% (w/v) sodium dodecyl sulfate (SDS, Sigma Steinheim, Germany) at 70°C for 30 min, and rinsed with DI water.

Blocking

In order to limit further non specific adsorption phenomena, a blocking step was performed by immersing the slide bearing DNA in 4% Bovine Serum Albumin (BSA, Sigma, Steinheim) solution for 2 h at 37°C. The slide was then washed in PBS 1 \times (pH 7.4)-Tween 20 at 0.05% for 3 \times 3min followed by PBS 1 \times (pH 7.4) 3 times, and finally rinsed with DI water and dried by centrifugation.

3-Biological recognition

Lectin labelling

Pseudomonas aeruginosa lectin I (noticed PA-IL provided by Dr. Anne Imberty, CERMAV) were labelled with Alexa647 by using a kit from Invitrogen. Protein concentration was estimated according to the manufacturer protocol by reading the absorbance at 280 and 650 nm. The final concentration of monomeric lectin was estimated at 7 μM with a degree of labeling of 1.6 for tetrameric PA-IL.

“In-solution” recognition

Glycomimetics (mixed or individually at 0.1, 0.5 or 1 μM final concentration) and lectin PA-IL (0.125 μM final concentration) were diluted in PBS-Tween 20 (0.02%) solution, BSA (2% final concentration) and CaCl_2 (1 $\mu\text{g}/\text{ml}$ final concentration). Each solution was pipetted down in its corresponding microwell of the slide and incubated 2h at 37°C in water saturated chamber. Finally the slide was washed with PBS 1 \times (pH 7.4)-Tween 20 (0.02%) for 5min and dried by centrifugation.

Fluorescence scanning

As mentioned before, three fluorochromes (see Table 2-5) were employed in this study. Cy3 was used to label glycoconjugates, whereas Cy5 and Alexa647 were used to label lectins. Thus the slides can be scanned with the Microarray scanner GenePix 4100A software package (Axon Instruments, Sunnyvale, USA) at excitation wavelengths of 532 and 635 nm. The fluorescence signal of each conjugate was determined as the average of the mean fluorescence signal of corresponding spots.

4-Figure for Hybridization and Cross Hybridization of the 7 glycomimetics.

All seven glycomimetics are labelled with Cy3 fluorophore. Each molecule was incubated individually in separated microwell. Each microwell displayed 56 spots corresponding to 8 repetition spots of the 7 immobilized DNA sequences and the negative sequence. Each DNA sequence is complementary to one of the DNA tag carried by one glycomimetic. In Figure 4, the Cy3 mean fluorescent of the mean signal of the eight spots is displayed as a function of the observed DNA spot.

Glycomimetic	Name of the DNA tag carried by each glycomimetic	Name of the complementary sequence covalently immobilized
G1	S1	CS1
G2	S2	CS2
G3	S3	CS3
G4	S4	CS4
G5	S5	CS5
G6	S6	CS6
G7	S7	CS7

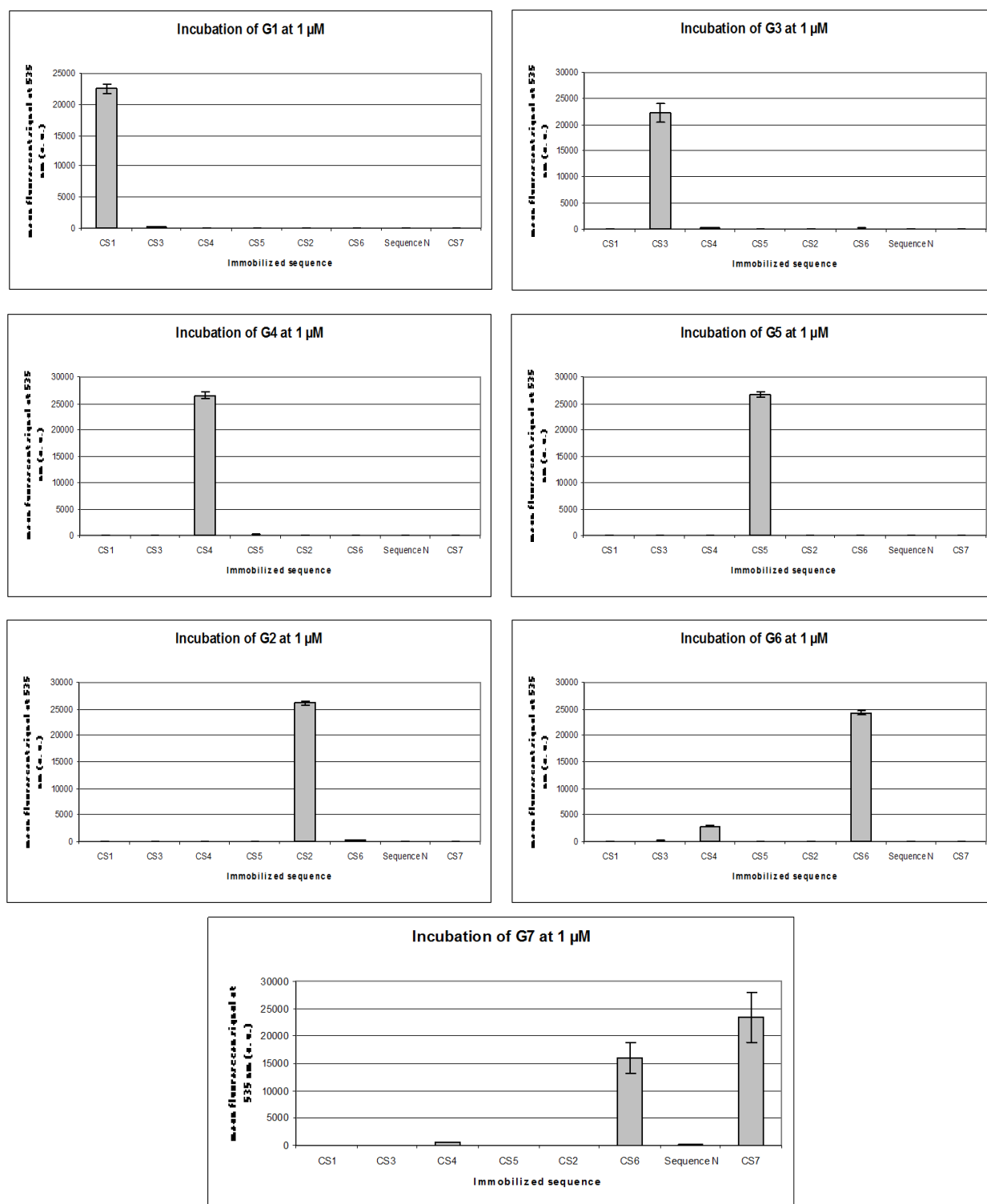


Figure 4. Mean Cy3 fluorescent signal as a function of the DNA sequence related spot.

5-Figure for Hybridization and Cross Hybridization of the 7 glycomimetics

Each glycomimetic was incubated individually in separated microwell with Alexa 647 labelled PA-IL (0.125 μM). Each microwell displayed 64 spots corresponding to 8 repetition

spots of the 7 immobilized DNA sequences and the negative sequence. Each DNA sequence is complementary to one of the DNA tag carried by one glycomimetic. In Figure 5, the Alexa 647 mean fluorescent of the mean signal of the eight spots is displayed as a function of the observed DNA spot.

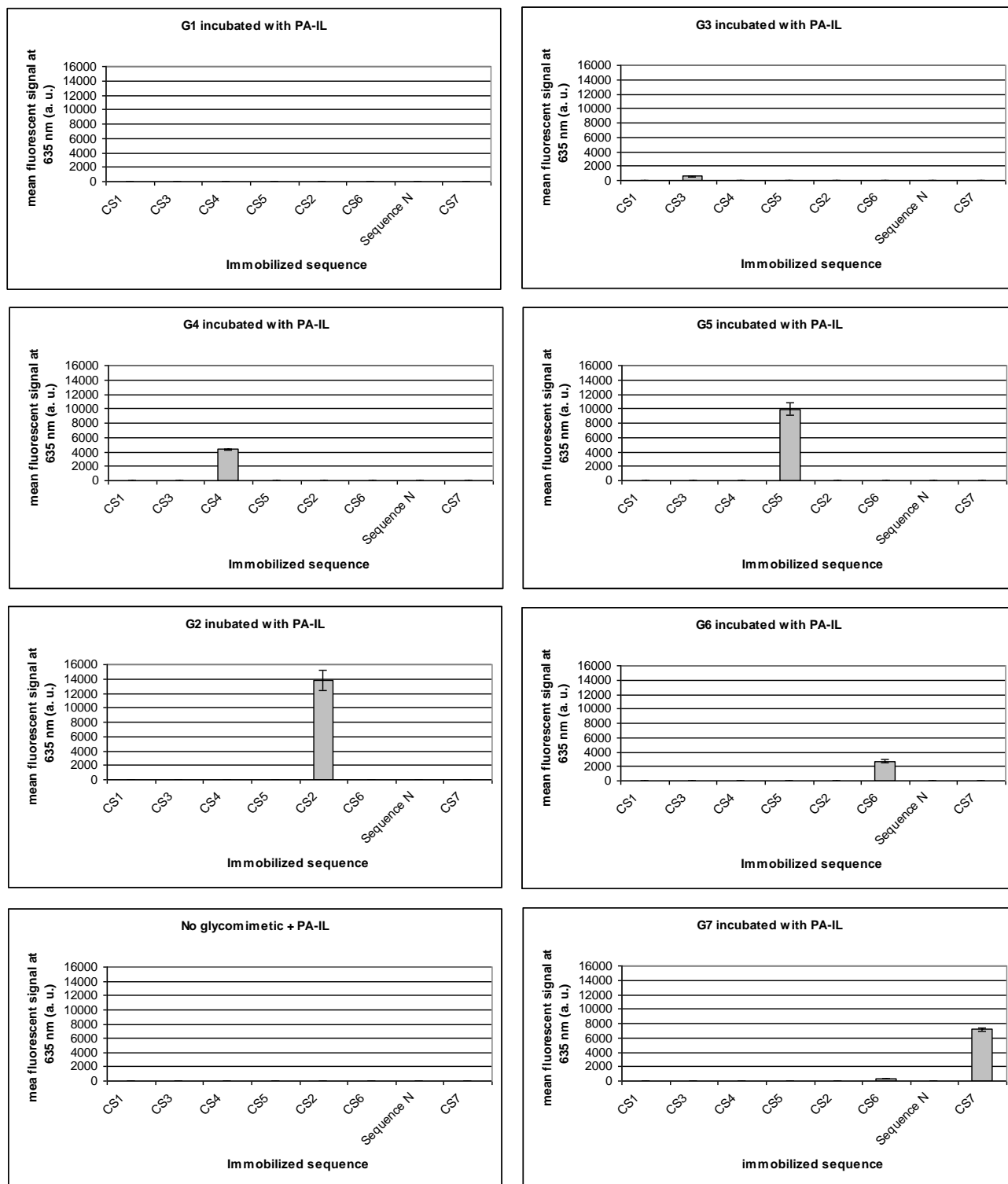


Figure 5. Mean Alexa 647 fluorescent signal as a function of the DNA sequence related spot.

6-F Molecular modelling protocol

Molecular modelling calculations were aimed at comparing **G2** and **G4**. While these two constructs are neutral, they exhibit a strong difference of affinity with PA-IL (4fold) in the microarray experiments. From a structural point of view, the arms bearing the galactoses are of different lengths for **G2** and **G4**.

The goal of our molecular modelling calculations was therefore to assess whether or not geometric specificities could explain the difference of affinity of **G2** and **G4** for the lectin. The calculations were performed for a simple configuration in which *one* construct interacts with *one* PA-IL. As previously discussed by Cecioni et al.,¹¹ tetravalent constructs may simultaneously interact with more than one lectin, thus leading to constructs/lectin aggregates. Exploring with molecular modelling these aggregates is beyond the scope of the present article, and would require far more modelling work.

We thus choose to focus on the comparison of potential energy of **G2/lectin** and **G4/lectin** complexes, for different numbers of bound galactoses.

The hypothesis for designing our calculations was that **G2** may exhibit arms long enough to enable binding of 3 galactoses of the same construct to one PA-IL (Fig.6 Left), while **G4** exhibits arms long enough to bind only 2 galactoses of the same construct to one PA-IL (Fig.6 right). Considering the structures of the constructs, it was unnecessary to consider the binding of 4 galactoses of a same construct onto one PA-IL.

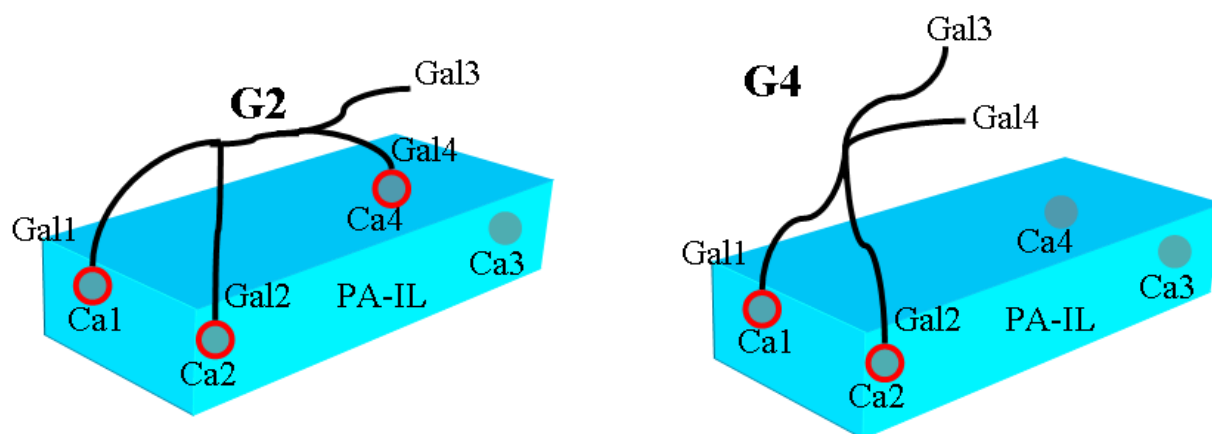


Figure 6. Hypothesis tested in the molecular modelling calculations

After building models of the glycoconjugates **G2** and **G4**, partial atomic charges were calculated by semi-empiric calculation. PA-IL model was prepared from X-ray structure (PDB code: 1OKO) after removal of the carbohydrate ligands and addition of hydrogen atoms. For each glycoconjugate, coordinates of three galactoses were overlaid and restrained to the coordinates of three of the initial galactose residues of 1OKO. Energy of the system

glycoconjugate + PA-IL was then minimized using firstly steepest-descent and secondly conjugated gradient calculations, with the Hyperchem/Mm+ force field, an extension of MM2.^{12, 13} Simulated annealing was performed on **G2** and **G4** for different constraints of the galactoses residues, to explore global conformational minima. Four types of restraints A, B, C, D were applied to the glycoconjugates (Fig.7):

- A) Gal1, Gal2, Gal3 ;
- B) Gal1, Gal2 ;
- C) Gal1 ;
- D) no constraint.

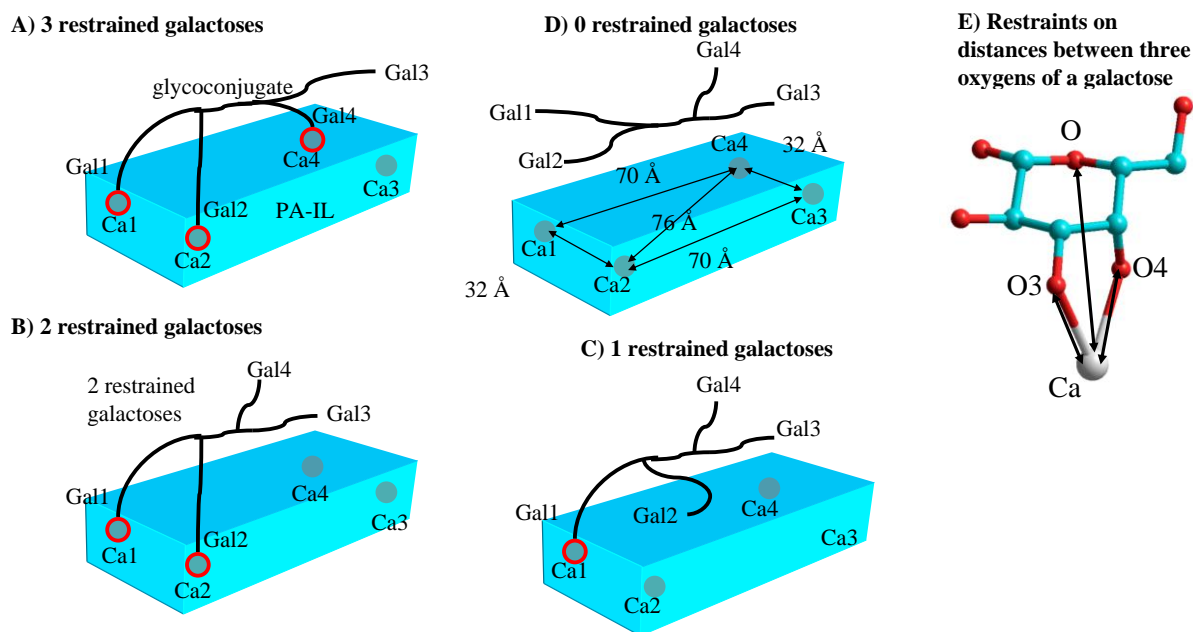


Figure 7. Location of constraints on galactose residues for simulated annealing. Distances indicated in D) and distances used for constraints in E) are obtained from 1OKO pdb model.

Constraints were applied between three oxygens of galactoses^{11, 14} and the calcium ion of their corresponding binding site (Fig.7 E). After an initial heating from 100 K to 390 K during 0.1 ps, annealing was performed at 390 K during 0.5 ps, followed by a cooling step of 0.5 ps to 90 K. The temperature was kept constant by coupling to a heat bath, with a relaxation time of 0.1 ps. Calculations were performed with a temperature step of 30 K and a time step of 0.0005 ps. The coordinates of the glycoconjugates atoms were saved every 5 fs during the simulation. Glycoconjugate potential energy and distances between O galactoses were monitored during simulated annealing for **G4** (Fig.8) and **G2** (Fig.9). Distances between O3 of galactoses were also monitored.

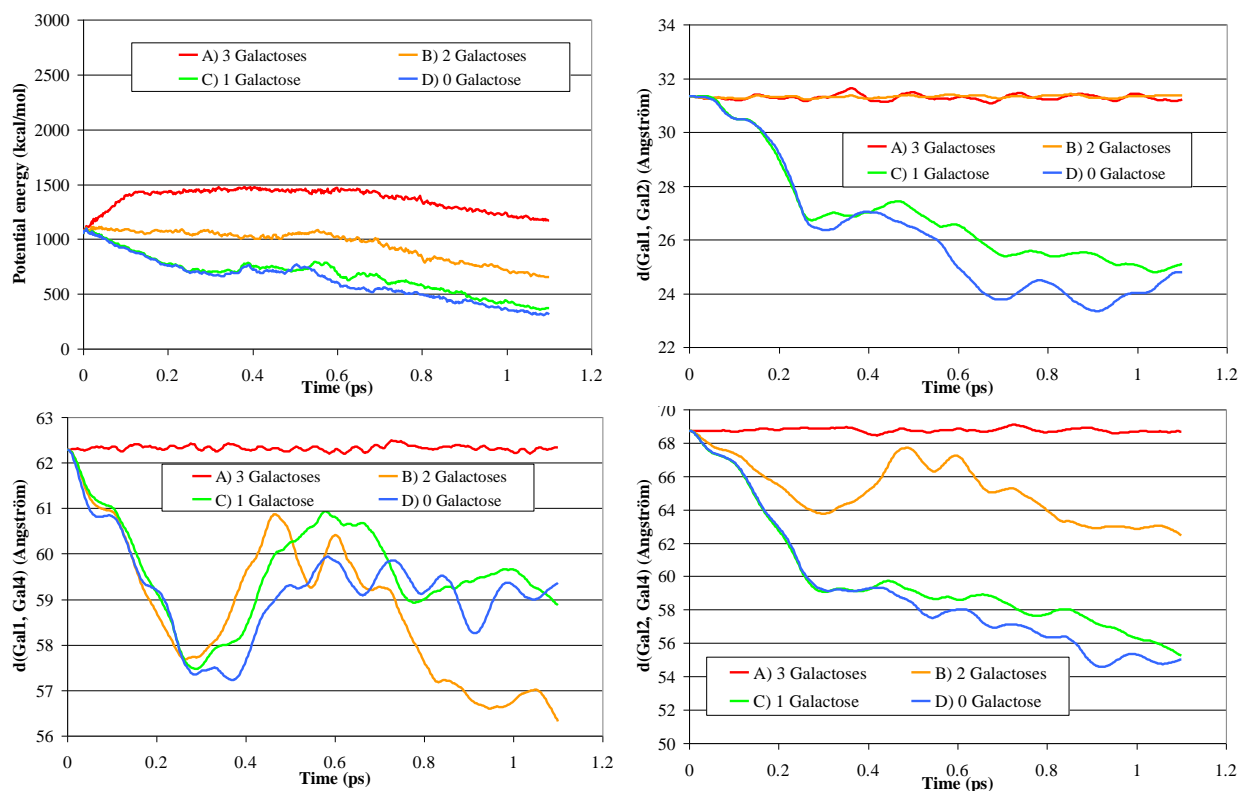


Figure 8. **G4**: results of simulated annealing. Potential energy versus time (top left), distance between galactoses versus time (top right: Gal1-Gal2; bottom-left: Gal1-Gal4; bottom-right: Gal2-Gal4) during simulated annealing of **G4**.

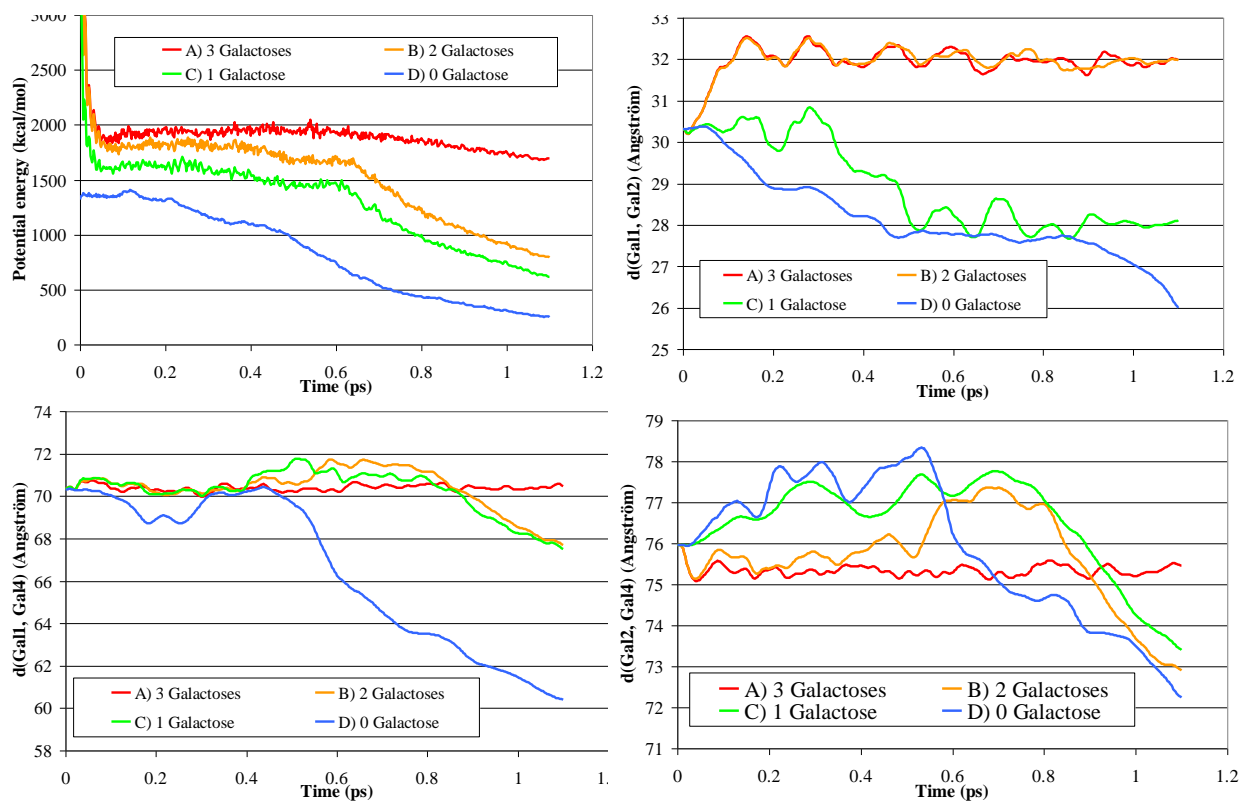


Figure 9. **G2**: results of simulated annealing. Potential energy versus time (top left), distance between galactoses versus time (top right: Gal1-Gal2 ; bottom-left: Gal1-Gal4; bottom-right: Gal2-Gal4) during simulated annealing of **G4**.

Potential energies of **G2** and **G4** are at least two-fold higher for configuration A (3 constrained galactoses) than for configuration B (2 constrained galactoses), as summarized in Fig.10. **G2** and **G4** are unlikely to interact with 3 galactoses to PA-IL. Differences of potential energy are less important between B and C configurations. Calculations seem to yield no evident difference between **G2** and **G4**.

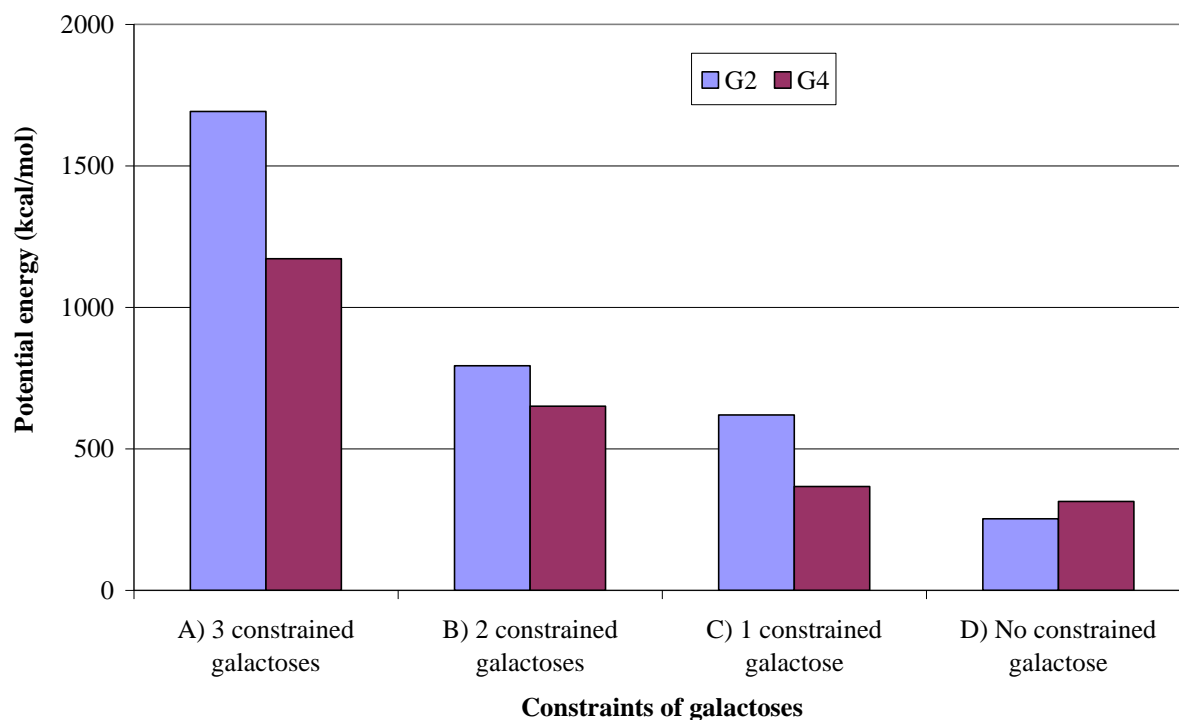


Figure 10. potential energy of **G2** and **G4** after simulated annealing, for different constraints.

Conclusion: The results of the present molecular modelling calculations seem to invalidate the hypothesis of Fig.6, because both **G2** and **G4** are unlikely to bind to 3 sites of PA-IL through 3 galactoses. Moreover, no significant energy differences seem to distinguish **G2** and **G4** when 2 galactoses of the constructs are bound to one PA-IL.

Performed calculations only enable here to compare the effect of the construct geometries on the stability of construct/PA-IL complexes, for several constrained configurations, when one tetravalent construct is bound to one PA-IL. The calculations give no information about docking of with PA-IL. Deeper calculations therefore should be performed in order to explain the difference of affinity of **G2** and **G4** with PA-IL. It will be necessary to take into account other parameters such as aggregates formation, docking of galactoses and interactions of construct arms with PA-IL on other sites than galactoses.

1. J. Lietard, A. Meyer, J. J. Vasseur and F. Morvan, *J. Org. Chem.*, 2008, **73**, 191-200.
2. F. Morvan, A. Meyer, A. Jochum, C. Sabin, Y. Chevolot, A. Imberty, J. P. Praly, J. J. Vasseur, E. Souteyrand and S. Vidal, *Bioconjug. Chem.*, 2007, **18**, 1637-1643.
3. C. Bouillon, A. Meyer, S. Vidal, A. Jochum, Y. Chevolot, J. P. Cloarec, J. P. Praly, J. J. Vasseur and F. Morvan, *J. Org. Chem.*, 2006, **71**, 4700-4702.
4. G. Pourceau, A. Meyer, J. J. Vasseur and F. Morvan, *J. Org. Chem.*, 2008, **73**, 6014-6017.
5. Z. Szurmai, L. Szabo and A. Liptak, *ACH Models Chem.*, 1989, **126**, 259-269.
6. Y. Chevolot, C. Bouillon, S. Vidal, F. Morvan, A. Meyer, J. P. Cloarec, A. Jochum, J. P. Praly, J. J. Vasseur and E. Souteyrand, *Angew. Chem. Int. Ed.*, 2007, **46**, 2398-2402.
7. R. Mazurczyk, G. E. Khoury, V. Dugas, B. Hannes, E. Laurenceau, M. Cabrera, S. Krawczyk, E. Souteyrand, J. P. Cloarec and Y. Chevolot, *Sens. Actuators, B*, 2008, **128**, 552-559.
8. J. Vieillard, R. Mazurczyk, C. Morin, B. Hannes, Y. Chevolot, P.-L. Desbène and S. Krawczyk, *J. Chromatogr. B*, 2007, **845**, 218-225.
9. V. Dugas and Y. Chevalier, *J. Colloid Interface Sci.*, 2003, **264**, 354-361.
10. V. Dugas, G. Depret, B. Chevalier, X. Nesme and E. Souteyrand, *Sens. Actuators, B*, 2004, **101**, 112-121.
11. S. Cecioni, R. Lalor, B. Blanchard, J. P. Praly, A. Imberty, S. E. Matthews and S. Vidal, *Chem.-Eur. J.*, 2009, **15**, 13232-13240.
12. N. L. Allinger, *J. Am. Chem. Soc.*, 1977, **99**, 8127-8134.
13. N. L. Allinger and Y. H. Yuh, *Quantum Chemistry Program Exchange, Bloomington, Indiana, Program No. 395, Molecular Mechanics*, American Chemical Society, Washington, D.C., 1982.
14. G. Cioci, E. P. Mitchell, C. Gautier, M. Wimmerova, D. Sudakevitz, S. Perez, N. Gilboa-Garber and A. Imberty, *FEBS Lett.*, 2003, **555**, 297-301.